

## CHARACTERIZING PERFORMANCE OF MULTIBAND UWB SYSTEMS USING POISSON CLUSTER ARRIVING FADING PATHS

*W. Pam Siritwongpairat*

Department of ECE  
University of Maryland,  
College Park, MD 20742  
Email: wipawee@eng.umd.edu

*Weifeng Su*

Department of Electrical Engineering  
State University of New York at Buffalo  
Buffalo, NY 14260  
Email: weifeng@eng.buffalo.edu

*K. J. Ray Liu*

Department of ECE  
University of Maryland,  
College Park, MD 20742  
Email: kjrlui@eng.umd.edu

### ABSTRACT

This paper provides a novel performance formulation for UWB systems that successfully captures the unique multipath-rich property and random-clustering phenomenon of UWB channels. Using the Saleh-Valenzuela model, we are able to characterize the pairwise error probability (PEP) performance for UWB systems employing multiband OFDM based on cluster arrival rate, ray arrival rate within a cluster, and cluster and ray decay factors. In addition, a PEP approximation technique is established, which allows us to obtain a closed-form PEP formulation that provides insightful understanding of the effect of channel characteristics on the performances of UWB systems. Finally, simulation results are provided to support the theoretical analysis.

### 1. INTRODUCTION

Ultra-wideband (UWB) has emerged as a technology that offers great promises to satisfy the growing demand for low cost and high-speed digital wireless home networks. UWB is generally defined as any transmission that occupies a bandwidth of more than 20% of its center frequency, or more than 500 MHz. Such ultra-wide bandwidth gives rise to important differences between UWB and narrowband channels, especially with respect to the number of resolvable paths and arrival times of multipath components [1]. In particular, the large bandwidth of UWB waveform considerably increases the receiver ability to resolve different reflections in UWB channel. As a result, the received signal contains a significant number of resolvable multipath components. Additionally, due to the very fine time resolution of UWB waveform, the multipath components tend to occur in cluster rather than in a continuum, as is common for narrowband channels.

In recent years, performance analysis of UWB systems has been an area of considerable interest. A number of UWB performances have been published in the literature (see [2] and references therein). However, most of them are based on the stochastic tapped-delay-line (STDL) models [3] used in conventional narrowband/wideband systems. Performance analysis in STDL models is basically an extension of that for narrowband systems, and it does not reflect the multipath-rich or random-clustering characteristics of UWB channels. To the best of our knowledge, none of the existing analysis is

insightful in revealing the effect of these unique characteristics to UWB system performances.

In order to implement an efficient UWB system, it is vital to capture the behavior of UWB channels. This motivates us to take into account the multipath-rich and clustering characteristics by using the Saleh-Valenzuela (S-V) model [4], where the multipath components randomly arrive in cluster. In the S-V model, the multipath arrivals are grouped into cluster arrivals and ray arrivals within each cluster. Both cluster and ray arrival times are modeled by statistical random processes based on Poisson process. The cluster and ray arrival rates depend on particular environments. This S-V model is shown by the IEEE 802.15.3a Task Group [5] to best fit the realistic UWB channel measurements.

In this paper, we analyze the performance of UWB systems that employ multiband orthogonal frequency division multiplexing (OFDM) [6]. Using the S-V model, we characterize the UWB performance in terms of cluster arrival rate, ray arrival rate, and cluster and ray decay factors. We provide at first an exact pairwise error probability (PEP) formulation for multiband UWB systems. Then, we establish an approximation approach, which allows us to obtain a closed-form PEP formulation. It turns out that the uncoded multiband system cannot gain from the multipath-clustering property of UWB channel. On the other hand, jointly encoding the data across subcarriers yields performance improvement, which strongly depends on cluster and ray arrival rates. Simulation results are provided to support the theoretical analysis.

### 2. SYSTEM MODEL

We consider a peer-to-peer multiband OFDM system [6] as proposed in the IEEE 802.15.3a standard [5]. The multiband approach divides the available UWB spectrum into several subbands, each with bandwidth of at least 500 MHz. The data is modulated using OFDM with  $N$  subcarriers, and one subband is used per transmission. The modulated OFDM symbols can be time-interleaved across various subbands [6].

#### 2.1. Channel Model

The channel model specified in the IEEE 802.15.3a standard [1] is based on the S-V model for indoor channels [4]. In S-V model, the channel impulse response can be modeled by

$$h(t) = \sum_{c=0}^C \sum_{l=0}^L \alpha_{c,l} \delta(t - T_c - \tau_{c,l}), \quad (1)$$

This work was supported in part by U.S. Army Research Laboratory under Cooperative Agreement DAAD 190120011.

where  $\alpha_{c,l}$  denotes the gain of the  $l^{\text{th}}$  multipath component in the  $c^{\text{th}}$  cluster. The time duration  $T_c$  represents the delay of the  $c^{\text{th}}$  cluster, and  $\tau_{c,l}$  is the delay of the  $l^{\text{th}}$  path in the  $c^{\text{th}}$  cluster relative to the cluster arrival time. The cluster arrivals and the path arrivals within each cluster can be modeled as Poisson distribution with rate  $\Lambda$  and rate  $\lambda$  ( $\lambda > \Lambda$ ), respectively. The path amplitude  $|\alpha_{c,l}|$  follows the log-normal, Nakagami, or Rayleigh distributions [1], whereas the phase  $\angle\alpha_{c,l}$  is uniformly distributed over  $[0, 2\pi)$ . For analytical tractability and to obtain insight understanding of UWB systems, we consider the scenario that the path amplitude  $|\alpha_{c,l}|$  is modeled as Rayleigh distribution [1], [7]. Specifically, the multipath gain coefficients  $\alpha_{c,l}$ 's are modeled as zero-mean, complex Gaussian random variables with variances [1]

$$\Omega_{c,l} = \text{E} [|\alpha_{c,l}|^2] = \Omega_{0,0} \exp\left(-\frac{T_c}{\Gamma} - \frac{\tau_{c,l}}{\gamma}\right), \quad (2)$$

where  $\text{E}[\cdot]$  stands for the expectation operation.  $\Omega_{0,0}$  is the mean energy of the first path of the first cluster,  $\Gamma$  is the cluster decay factor, and  $\gamma$  is the ray decay factor. The powers of the multipath components are normalized such that  $\sum_{c=0}^C \sum_{l=0}^L \Omega_{c,l} = 1$ . The channel parameters corresponding to several scenarios are provided in [1]. From (1), the channel frequency response is given by

$$H(f) = \sum_{c=0}^C \sum_{l=0}^L \alpha_{c,l} \exp(-j2\pi f(T_c + \tau_{c,l})), \quad (3)$$

where  $j \triangleq \sqrt{-1}$ .

## 2.2. Signal Model

With the choice of cyclic prefix length greater than the duration of the channel impulse response, OFDM allows for each UWB subband to be divided into a set of  $N$  orthogonal narrowband channels. At the transmitter, an information sequence is partitioned into blocks. Each block is mapped onto an  $N \times 1$  matrix  $\mathbf{D} = [d(0) d(1) \cdots d(N-1)]^T$ , where  $d(n)$ ,  $n = 0, 1, \dots, N-1$ , represents a complex symbol to be transmitted over subcarrier  $n$ . The matrix  $\mathbf{D}$  is normalized to have average energy  $\text{E} [\|\mathbf{D}\|^2] = N$ , where  $\|\cdot\|$  denotes the Frobenius norm [8]. Suppose the information is jointly encoded across  $S$  ( $1 \leq S \leq N$ ) subcarriers. In particular, the data matrix  $\mathbf{D}$  is a concatenation of  $P = \lfloor N/S \rfloor$  data matrices as follows:

$$\mathbf{D} = \begin{bmatrix} \mathbf{D}_0^T & \mathbf{D}_1^T & \cdots & \mathbf{D}_{(P-1)}^T & \mathbf{0}_{(N-PS) \times 1} \end{bmatrix}^T, \quad (4)$$

where  $\mathbf{D}_p = [d_p(0) d_p(1) \cdots d_p(S-1)]^T$  with  $d_p(s) \triangleq d(pS + s)$  for  $p = 0, 1, \dots, P-1$  is a data matrix of size  $S \times 1$ , and  $\mathbf{0}_{m \times n}$  stands for an  $m \times n$  all-zero matrix. The data matrices  $\mathbf{D}_p$ 's are independently designed for different  $p$ , and the energy constraint satisfies  $\text{E} [\|\mathbf{D}_p\|^2] = S$  for all  $p$ . The transmitter applies  $N$ -point IFFT to the matrix  $\mathbf{D}$ , appends a cyclic prefix and guard interval, up-converts to RF, and then sends the modulated signal at each subcarrier.

At the receiver, after matched filtering, removing the cyclic prefix, and applying FFT, the received signal at the  $n^{\text{th}}$  subcarrier is given by

$$y(n) = \sqrt{E_s} d(n) H(n) + z(n), \quad (5)$$

where  $E_s$  is the average transmitted energy per symbol,

$$H(n) = \sum_{c=0}^C \sum_{l=0}^L \alpha_{c,l} \exp(-j2\pi n \Delta f (T_c + \tau_{c,l})) \quad (6)$$

is the frequency response of the channel at subcarrier  $n$ ,  $\Delta f = 1/T$  is the frequency separation between two adjacent subcarriers, and  $T$  is the OFDM symbol period. In (5),  $z(n)$  represents the noise sample at the  $n^{\text{th}}$  subcarrier. We model  $z(n)$  as complex Gaussian random variable with zero mean and variance  $N_0$ . The channel state information  $H(n)$  is assumed known at the receiver, but not at the transmitter.

## 3. PERFORMANCE ANALYSIS

In this section, we first present a general framework to analyze the performance of multiband UWB systems. Then, using the S-V model, we characterize the average PEP of multiband UWB systems based on cluster and ray arrival rates.

For subsequent performance evaluation, we format the received signal in (5) in a matrix form as

$$\mathbf{Y}_p = \sqrt{E_s} X(\mathbf{D}_p) \mathbf{H}_p + \mathbf{Z}_p, \quad (7)$$

where  $X(\mathbf{D}_p) = \text{diag}(d_p(0), d_p(1), \dots, d_p(S-1))$  is an  $S \times S$  diagonal matrix with the elements of  $\mathbf{D}_p$  on its main diagonal. The channel matrix  $\mathbf{H}_p$ , the received signal matrix  $\mathbf{Y}_p$ , and the noise matrix  $\mathbf{Z}_p$  have the same forms as  $\mathbf{D}_p$  by replacing  $d$  with  $H$ ,  $y$  and  $z$ , respectively. The receiver exploits a maximum likelihood decoder, where the decoding process is jointly performed within each data matrix  $\mathbf{D}_p$ , and the decision rule can be stated as

$$\hat{\mathbf{D}}_p = \arg \min_{\mathbf{D}_p} \|\mathbf{Y}_p - \sqrt{E_s} X(\mathbf{D}_p) \mathbf{H}_p\|^2. \quad (8)$$

Suppose that  $\mathbf{D}_p$  and  $\hat{\mathbf{D}}_p$  are two distinct data matrices. Since the data matrices  $\mathbf{D}_p$ 's for different  $p$  are independently en/decoded, for simplicity, the PEP can be defined as the probability of erroneously decoding the matrix  $\hat{\mathbf{D}}_p$  when  $\mathbf{D}_p$  is transmitted. Following the computation steps as in [3], the average PEP, denoted as  $P_e$ , is given by

$$P_e = \text{E} \left[ \text{Q} \left( \sqrt{\frac{\rho}{2}} \|\Delta_p \mathbf{H}_p\|^2 \right) \right], \quad (9)$$

where  $\rho = E_s/N_0$  is the average signal-to-noise ratio (SNR),  $\Delta_p = X(\mathbf{D}_p) - X(\hat{\mathbf{D}}_p)$ , and  $\text{Q}(x) = \frac{1}{\sqrt{2\pi}} \int_x^\infty \exp(-\frac{t^2}{2}) dt$  is the Gaussian error function. Denoting

$$\eta = \|\Delta_p \mathbf{H}_p\|^2, \quad (10)$$

and using an alternate representation of Q function [9],  $\text{Q}(x) = \frac{1}{\pi} \int_0^{\pi/2} \exp(-\frac{x^2}{2 \sin^2 \theta}) d\theta$  for  $x \geq 0$ , the average PEP in (9) can be expressed as

$$P_e = \frac{1}{\pi} \int_0^{\pi/2} \mathcal{M}_\eta \left( -\frac{\rho}{4 \sin^2 \theta} \right) d\theta, \quad (11)$$

where  $\mathcal{M}_\eta(u) = \mathbb{E}[\exp(u\eta)]$  represents the moment generating function (MGF) of  $\eta$  [9]. From (11), we can see that the remaining problem is to obtain the MGF  $\mathcal{M}_\eta(u)$ .

For convenience, let us denote a  $(C+1)(L+1) \times 1$  channel matrix  $\mathbf{A} = [\alpha_{0,0} \cdots \alpha_{0,L} \cdots \alpha_{C,0} \cdots \alpha_{C,L}]^T$ . According to (6),  $\mathbf{H}_p$  can be decomposed as  $\mathbf{H}_p = \mathbf{W}_p \cdot \mathbf{A}$ , where  $\mathbf{W}_p$  is an  $S \times (C+1)(L+1)$  matrix, defined as

$$\mathbf{W}_p = \begin{pmatrix} \omega_{p,0}^{T_0+\tau_{0,0}} & \omega_{p,0}^{T_0+\tau_{0,1}} & \cdots & \omega_{p,0}^{T_C+\tau_{C,L}} \\ \omega_{p,1}^{T_0+\tau_{0,0}} & \omega_{p,1}^{T_0+\tau_{0,1}} & \cdots & \omega_{p,1}^{T_C+\tau_{C,L}} \\ \vdots & \vdots & \ddots & \vdots \\ \omega_{p,S-1}^{T_0+\tau_{0,0}} & \omega_{p,S-1}^{T_0+\tau_{0,1}} & \cdots & \omega_{p,S-1}^{T_C+\tau_{C,L}} \end{pmatrix},$$

in which  $\omega_{p,s} \triangleq \exp(-j2\pi \Delta f (pS + s))$ . After some manipulations, we can rewrite  $\eta$  in (10) as

$$\eta = \sum_{s=1}^S \text{eig}_s(\Psi) |\beta_s|^2, \quad (12)$$

where  $\beta_s$ 's are identically independent distributed (iid) complex Gaussian random variables with zero mean and unit variance, and  $\text{eig}_s(\Psi)$ 's are the eigenvalues of matrix

$$\Psi = \Omega^{\frac{1}{2}} \mathbf{W}_p^H \Delta_p^H \Delta_p \mathbf{W}_p \Omega^{\frac{1}{2}}. \quad (13)$$

In (13),  $(\cdot)^H$  denotes conjugate transpose operation, and  $\Omega = \text{diag}(\Omega_{0,0}, \Omega_{0,1}, \dots, \Omega_{C,L})$  is a diagonal matrix formed from the average powers of multipath components. From (12), the MGF of  $\eta$  is given by

$$\mathcal{M}_\eta(u) = \mathbb{E} \left[ \prod_{s=1}^S (1 - u \text{eig}_s(\Psi))^{-1} \right]. \quad (14)$$

Observe that the eigenvalues  $\text{eig}_s(\Psi)$ 's depend on  $T_c$ 's and  $\tau_{c,l}$ 's which are based on Poisson process. Generally, it is difficult, if not impossible, to determine  $\mathcal{M}_\eta(u)$  in (14). However, for uncoded multiband system, i.e., the number of jointly encoded subcarriers  $S = 1$ , we have the following result.

**Theorem 1** *When there is no coding across subcarriers, the average PEP is given by*

$$P_e = \frac{1}{\pi} \int_0^{\pi/2} \left( 1 + \frac{\rho}{4 \sin^2 \theta} |d - \hat{d}|^2 \right)^{-1} d\theta, \quad (15)$$

for any channel parameters.

*Proof.* In case of no coding, the nonzero eigenvalue of matrix  $\Psi$  in (13) is

$$\text{eig}(\Psi) = |d - \hat{d}|^2 \text{eig}(\mathbf{W}_p \Omega \mathbf{W}_p^H) = |d - \hat{d}|^2. \quad (16)$$

The second equality in (16) follows from the fact that the matrix  $\mathbf{W}_p \Omega \mathbf{W}_p^H = \sum_{c=0}^C \sum_{l=0}^L \Omega_{c,l} = 1$ . Substitute  $\text{eig}(\Psi) = |d - \hat{d}|^2$  into (14), and then substitute the resulted MGF into the PEP formulation in (11), yielding the average PEP in (15).  $\square$

The result in Theorem 1 is somewhat surprising since the performance of uncoded multiband UWB system does not depend on multipath arrival rates or decay factors. In addition, the performance of UWB system is the same as that of narrowband system in Rayleigh fading environment. This implies that we cannot gain from the multipath-rich and random-clustering properties of UWB channel if the data is not encoded across subcarriers.

#### 4. APPROXIMATE PEP FORMULATION

In this section, we establish an approximation approach which allows us to provide a closed-form PEP formulation when the information is jointly encoded across subcarriers.

Observe from (10) that  $\eta = (\Delta_p \mathbf{H}_p)^H \Delta_p \mathbf{H}_p$  is in a quadratic form. Using a representation of quadratic form in ([10], p.29), and noting that  $\mathbb{E}[\Delta_p \mathbf{H}_p] = \mathbf{0}$ , we can approximate  $\eta$  by

$$\eta \approx \sum_{s=1}^S \text{eig}_s(\Phi) |\mu_s|^2, \quad (17)$$

where  $\mu_s$ 's are iid zero-mean Gaussian random variables with unit variance, and

$$\Phi = \mathbb{E}[\Delta_p \mathbf{H}_p (\Delta_p \mathbf{H}_p)^H] = \Delta_p \mathbf{R} \Delta_p^H, \quad (18)$$

in which  $\mathbf{R} = \mathbb{E}[\mathbf{H}_p \mathbf{H}_p^H]$ . Let the eigenvalues,  $\text{eig}_s(\Phi)$ 's, be arranged in a non-increasing order as:  $\text{eig}_1(\Phi) \geq \text{eig}_2(\Phi) \cdots \geq \text{eig}_S(\Phi)$ . By Ostrowski's theorem ([8], p.224), the eigenvalues of  $\Phi$  are given by

$$\text{eig}_s(\Phi) = \text{eig}_s(\Delta_p \mathbf{R} \Delta_p^H) = \nu_s \text{eig}_s(\mathbf{R}), \quad (19)$$

where  $\nu_s$  is a nonnegative real number that satisfies  $\text{eig}_S(\Delta_p \Delta_p^H) \leq \nu_s \leq \text{eig}_1(\Delta_p \Delta_p^H)$  for  $s = 1, 2, \dots, S$ . From this alternative approach, we are able to approximate the average PEP as follows.

**Theorem 2** *When the information is jointly encoded across  $S$  ( $1 \leq S \leq N$ ) subcarriers, the average PEP can be approximated as*

$$P_e \approx \frac{1}{\pi} \int_0^{\pi/2} \prod_{s=1}^S \left( 1 + \frac{\rho \nu_s}{4 \sin^2 \theta} \text{eig}_s(\mathbf{R}) \right)^{-1} d\theta, \quad (20)$$

where the  $S \times S$  matrix  $\mathbf{R}$  is given by

$$\mathbf{R} = \begin{pmatrix} 1 & R(1)^* & \cdots & R(S-1)^* \\ R(1) & 1 & \cdots & R(S-2)^* \\ \vdots & \vdots & \ddots & \vdots \\ R(S-1) & R(S-2) & \cdots & 1 \end{pmatrix}, \quad (21)$$

and  $R(s)$ 's for  $s = 1, 2, \dots, S$  are defined as

$$R(s) = \Omega_{0,0} \frac{\Lambda + g(\frac{1}{T}, s)}{g(\frac{1}{T}, s)} \frac{\lambda + g(\frac{1}{\gamma}, s)}{g(\frac{1}{\gamma}, s)}, \quad (22)$$

in which  $g(a, s) \triangleq a + j2\pi s \Delta f$ .

*Proof.* By substituting (19) into (17) and then using the MGF of the approximate  $\eta$ , we obtain the approximate PEP in (20). Observe that the  $(n, n')^{th}$  entry of matrix  $\mathbf{R}$  is  $E[H(n)H(n')^*]$  for  $0 \leq n, n' \leq S-1$ . The elements on the main diagonal of  $\mathbf{R}$  are given by

$$R(n, n) = E[|H(n)|^2] = \sum_{c=0}^C \sum_{l=0}^L E[|\alpha_{c,l}|^2] = 1. \quad (23)$$

The off-diagonal elements of  $\mathbf{R}$ ,  $R(n, n')$ 's for  $n \neq n'$ , can be evaluated as follows:

$$\begin{aligned} R(n, n') &= E[H(n)H(n')^*] \\ &= \sum_{c=0}^C \sum_{l=0}^L E \left[ E[|\alpha_{c,l}|^2] e^{-j2\pi(n-n')\Delta f(T_c + \tau_{c,l})} \right] \\ &\triangleq R(n - n'). \end{aligned} \quad (24)$$

Substitute (2) into (24), resulting in

$$R(s) = \sum_{c=0}^C \sum_{l=0}^L \Omega_{0,0} G_{c,l}(s), \quad (25)$$

where

$$G_{c,l}(s) = E \left[ \exp \left( -g \left( \frac{1}{\Gamma}, s \right) T_c - g \left( \frac{1}{\gamma}, s \right) \tau_{c,l} \right) \right]. \quad (26)$$

To calculate  $G_{c,l}(s)$  in (26), we denote  $x_i$  as an inter-arrival time between clusters  $i$  and  $i-1$ . According to the Poisson distribution of the cluster delays,  $x_i$ 's can be modeled as iid exponential random variables with parameter  $\Lambda$ , and the delay of the  $c^{th}$  cluster,  $T_c$ , can be expressed as  $T_c = \sum_{i=0}^c x_i$ . Similarly, let  $v_{c,j}$  denote an inter-arrival time between rays  $j$  and  $j-1$  in the  $c^{th}$  cluster. We can also model  $v_{c,j}$ 's as iid exponential random variables with parameter  $\lambda$ , and the delay of the  $l^{th}$  path within cluster  $c$  can be given by  $\tau_{c,l} = \sum_{j=0}^l v_{c,j}$ . By re-writing  $G_{c,l}(s)$  in terms of  $x_i$  and  $v_{c,j}$ , (26) can be simplified to

$$\begin{aligned} G_{c,l}(s) &= E \left[ \prod_{i=0}^c e^{-g(\frac{1}{\Gamma}, s)x_i} \right] E \left[ \prod_{j=0}^l e^{-g(\frac{1}{\gamma}, s)v_{c,j}} \right] \\ &= \left( \frac{\Lambda}{\Lambda + g(\frac{1}{\Gamma}, s)} \right)^c \left( \frac{\lambda}{\lambda + g(\frac{1}{\gamma}, s)} \right)^l. \end{aligned} \quad (27)$$

Substituting (27) into (25), and using the fact that  $C$  and  $L$  are generally large, we obtain the result in (22).  $\square$

In the sequel, we provide the PEP approximations for the cases of no coding and jointly encoding across two subcarriers to get some insight understanding.

1. In case of no coding, i.e.,  $S = 1$ , the matrix  $\mathbf{R}$  in (21) reduces to  $\mathbf{R} = 1$ , and  $\nu_1 = |d - \hat{d}|^2$ . From (20), the approximate PEP is given by

$$P_e \approx \frac{1}{\pi} \int_0^{\pi/2} \left( 1 + \frac{\rho}{4 \sin^2 \theta} |d - \hat{d}|^2 \right)^{-1} d\theta. \quad (28)$$

2. When the information is jointly encoded across 2 subcarriers, i.e.,  $S = 2$ , the eigenvalues of matrix  $\mathbf{R}$  are  $1 + |R(1)|$  and  $1 - |R(1)|$ . Substituting these eigenvalues into (20), we obtain the approximate PEP

$$P_e \approx \frac{1}{\pi} \int_0^{\pi/2} \left( 1 + \frac{\rho J + \rho^2 \nu_1 \nu_2 (1 - B^2)}{16 \sin^4 \theta} \right)^{-1} d\theta, \quad (29)$$

where  $J = 4 \sin^2 \theta [\nu_1 + \nu_2 + B(\nu_1 - \nu_2)]$  and

$$B = \Omega_{0,0} \frac{[(\Lambda + \frac{1}{\Gamma})^2 + b]^{\frac{1}{2}} [(\lambda + \frac{1}{\gamma})^2 + b]^{\frac{1}{2}}}{[(\frac{1}{\Gamma})^2 + b]^{\frac{1}{2}} [(\frac{1}{\gamma})^2 + b]^{\frac{1}{2}}}, \quad (30)$$

and  $b = (2\pi\Delta f)^2$ . In UWB,  $b$  is normally much less than  $\frac{1}{\gamma^2}$  and  $\frac{1}{\Gamma^2}$ . Hence, (30) can be approximated by

$$B \approx \Omega_{0,0} (\Lambda\Gamma + 1)(\lambda\gamma + 1). \quad (31)$$

Observe that for uncoded multiband UWB system, the PEP obtained from the approximation approach in (28) is consistent with the exact PEP given in (15), which shows that multiband UWB performances do not depend on the clustering characteristic. In case of jointly encoding across multiple subcarriers, the PEPs in (20) and (29) reveal that multiband UWB performances depend on the correlations in the frequency response among different subcarriers,  $R(s)$ 's, which in turn relate to the path arrival rates and decay factors. For instance, suppose each data symbol  $d$  is transmitted repeatedly in two subcarriers, and channel model (CM) parameters follow those specified in the IEEE 802.15.3a channel modeling report [1]. Let  $\nu = |d - \hat{d}|^2$  and  $\Delta f = 4.125$  MHz, then the approximate PEP can be obtained from (29) as follows:

- With CM 1,  $\Lambda = 0.0233$ ,  $\lambda = 2.5$ ,  $\Gamma = 7.1$ ,  $\gamma = 4.3$ ,  $\Omega_{0,0} = 0.0727$ :  $P_e \approx \frac{1}{\pi} \int_0^{\frac{\pi}{2}} \left( 1 + \frac{\rho^2 \nu^2 0.0294}{16 \sin^4 \theta} \right)^{-1} d\theta$ .
- With CM 4,  $\Lambda = 0.0667$ ,  $\lambda = 2.1$ ,  $\Gamma = 24$ ,  $\gamma = 12$ ,  $\Omega_{0,0} = 0.0147$ :  $P_e \approx \frac{1}{\pi} \int_0^{\frac{\pi}{2}} \left( 1 + \frac{\rho^2 \nu^2 0.3026}{16 \sin^4 \theta} \right)^{-1} d\theta$ .

We can see from the above examples that UWB performance in CM 4 is better than that in CM 1. This comes from the fact that the multipath components in CM 4 are more random than those in CM 1, which implies that compared with CM 1, CM 4 has less correlation in the frequency response among different subcarriers, and hence yields better performance.

## 5. SIMULATION RESULTS

We performed simulations for a multiband UWB system with  $N = 128$  subcarriers and the subband bandwidth of 528 MHz. Our simulated channel model was based on (1) with the path gains  $\alpha_{c,l}$ 's being independent zero-mean complex Gaussian random variables with variances specified in (2). The channel model parameters followed those for CM 1 and CM 4 [1].

In our simulations, the data matrix  $\mathbf{D}$  in (4) were constructed via a repetition mapping. To be specific, each data

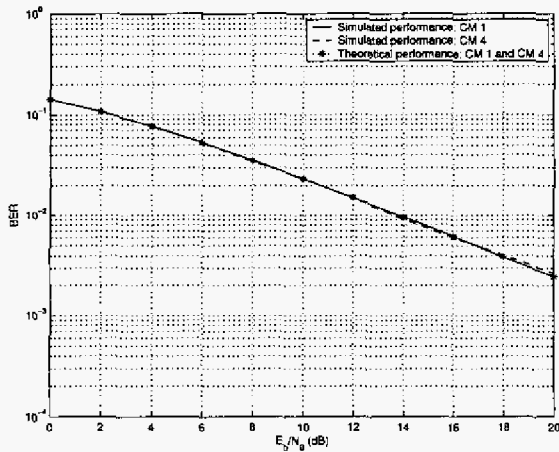


Fig. 1. Performances of multiband UWB system without coding.

matrix  $D_p$  contained only one information symbol  $d_p$ , i.e.,  $D_p = d_p \cdot \mathbf{1}_{S \times 1}$ , where  $\mathbf{1}_{m \times n}$  denotes an  $m \times n$  all-one matrix. The data symbols can be selected from BPSK or QPSK constellations. Here, we consider a multiband system with BPSK signals in which no channel coding was applied. In this case, the average PEP is equivalent to the bit-error-rate (BER) performance. Figures 1 and 2 illustrate the BER performances of multiband UWB systems as functions of the average SNR per bit ( $E_b/N_0$ ) in dB.

In Figure 1, we show the simulated and theoretical BER performances of multiband system without coding ( $S = 1$ ). We observe that the performances of UWB system in CM 1 and CM 4 are almost the same, and they are close to the exact PEP calculation in (15). The simulation results confirm the theoretical expectation that the performances of multiband UWB systems without coding across subcarriers are the same for every channel environment.

We also simulated the performances of multiband UWB system with the information jointly encoded across two subcarriers ( $S = 2$ ). In Figure 2, we compared the simulation results and the PEP approximation in (20). We can see that the theoretical approximations are close to the simulated performances for both CM 1 and CM 4. In addition, the performance obtained with CM 4 is superior to that with CM 1, which is in agreement with the theoretical results in the previous section. Figure 2 shows that the PEP approximations can well reflect the multipath-rich and random-clustering characteristics on the performances of UWB systems.

## 6. CONCLUSIONS

In this paper, we provided PEP performance analysis that captures the unique multipath-rich and clustering characteristics of UWB channels. First, a closed-form PEP formulation was obtained for the case of no coding across subcarriers. Interestingly, both theoretical and simulation results revealed that the performances of uncoded multiband UWB systems do not depend on the clustering property. Then, we obtained a PEP approximation in case when the data is jointly encoded

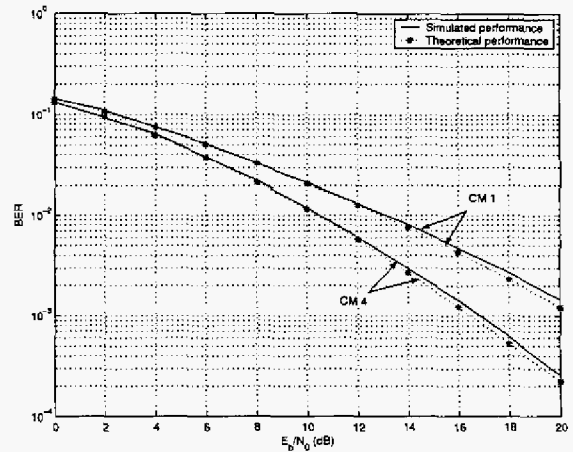


Fig. 2. Performances of multiband UWB system with jointly coding across two subcarriers.

across multiple subcarriers. The theoretical approximations revealed that UWB performances depend heavily on the correlations in the channel frequency response among different subcarriers, which in turn relate to the cluster arrival rate, ray arrival rate, and cluster and ray decay factors. Simulation results confirmed that the theoretical approximations can successfully capture the effect of random-clustering phenomenon on the performances of multiband UWB system.

## 7. REFERENCES

- [1] J. Foerster, et. al, "Channel Modeling Sub-committee Report Final", IEEE802.15-02/490, Nov. 18, 2003.
- [2] L. Yang and G. B. Giannakis, "Ultra-Wideband Communications: An Idea whose Time has Come," *IEEE Signal Processing Magazine*, vol. 21, no. 6, pp. 26-54, Nov. 2004.
- [3] J. G. Proakis, *Digital Communications*, 4<sup>th</sup> Ed., McGraw-Hill, New York, 2001.
- [4] A. A. M. Saleh and R. A. Valenzuela, "A Statistical Model for Indoor Multipath Propagation", *IEEE J. on Selected Areas in Commun.*, vol. 5, no. 2, pp. 128-137, Feb. 1987.
- [5] IEEE 802.15WPAN High Rate Alternative PHY Task Group 3a (TG3a). Internet: [www.ieee802.org/15/pub/TG3a.html](http://www.ieee802.org/15/pub/TG3a.html)
- [6] A. Batra, et. al, "Design of a Multiband OFDM System for Realistic UWB Channel Environments," *IEEE Trans. on Microwave Theory and Tech.*, vol. 52, no. 9, pp. 2123-2138, Sep. 2004.
- [7] R. J. Cramer, R. A. Scholtz, and M. Z. Win, "Evaluation of an Ultra-Wide-Band Propagation Channel", *IEEE Trans. on Antennas and Propagation*, vol. 50, pp. 561-570, May 2002.
- [8] R. A. Horn and C. R. Johnson, *Matrix Analysis*, Cambridge Univ. Press, New York, 1985.
- [9] M. K. Simon and M. S. Alouini, *Digital Communication over Fading Channels: A Unified Approach to Performance Analysis*, John Wiley and Sons, New York, 2000.
- [10] A. M. Mathai and S. B. Provost, *Quadratic Forms in Random Variables: Theory and Applications*, Marcel Dekker Inc., New York, 1992.